

# Surface behaviour of the pairing gap in a slab of nuclear matter

M. Baldo<sup>1</sup>, M. Farine<sup>2</sup>, U. Lombardo<sup>3,4</sup>, E. E. Saperstein<sup>5</sup>, P. Schuck<sup>6</sup>,  
and M. V. Zverev<sup>5</sup>

<sup>1</sup>*INFN, Sezione di Catania, 57 Corso Italia, I-95129 Catania, Italy*

<sup>2</sup>*Ecole Navale, Lanv oc-Poulmic, 29240 Brest-Naval, France*

<sup>3</sup>*INFN-LNS, 44 Via S.-Sofia, I-95123 Catania, Italy*

<sup>4</sup>*Dipartimento di Fisica, 57 Corso Italia, I-95129 Catania, Italy*

<sup>5</sup>*Kurchatov Institute, 123182, Moscow, Russia*

<sup>6</sup>*Insitut de Physique Nucl aire, IN2P3-CNRS,*

*Universit  Paris-Sud, F-91406 Orsay-C dex, France*

---

## Abstract

The surface behavior of the pairing gap previously studied for semi-infinite nuclear matter is analyzed in the slab geometry. The gap-shape function is calculated in two cases: (a) pairing with the Gogny force in a hard-wall potential and (b) pairing with the separable Paris interaction in a Saxon-Woods mean-field potential. It is shown that the surface features are preserved in the case of slab geometry, being almost independent of the width of the slab. It is also demonstrated that the surface enhancement is strengthened as the absolute value of chemical potential  $|\mu|$  decreases which simulates the approach to the nucleon drip line.

---

## 1. Introduction

Recently, the surface behavior of the pairing gap in the  $^1S_0$ -channel in semi-infinite nuclear matter was investigated independently from two quite different approaches [1], [2]. A rather sophisticated approach was used in [1] which starts from the microscopic gap equation for semi-infinite nuclear matter with the separable representation [3, 4] of the Paris potential [5]. The effective pairing interaction  $\mathcal{V}_{\text{eff}}^p$  adopted in the gap equation was previously found within the Bethe-Goldstone formalism for semi-infinite nuclear matter without any form of local approximation [6]. All the calculations were made for two values of the chemical potential:  $\mu = -16$  MeV and  $\mu = -8$  MeV. A surface enhancement in the gap  $\Delta$  was found, the effect being more pronounced for  $\mu = -8$  MeV.

In [2] a more simplified model was used in which nuclear matter was embedded in a semi-infinite hard wall potential and the pairing problem was considered in the BCS approximation with the Gogny force. Such a simple approach makes it possible to solve the problem to a great deal analytically and to examine the coordinate dependence of the pairing gap, pairing tensor and correlation energy density in a rather transparent way. A relatively mild surface enhancement of all the quantities under consideration was found. As to  $\Delta$ , it is of the same size as in [1].

In this paper we carried out an analogous analysis for a slab of nuclear matter within both approaches with the hope that a direct comparison of results can help to clarify the general features of the phenomenon under consideration. The slab system is much closer to real atomic nuclei than the semi-infinite one and many results can be qualitatively related to them.

The structure of the article is as follows. In Section 2 we extend the model with the Gogny force [2] to the case of a hard-wall slab potential. Section 3 contains the extension of the model of [1] with the Paris force to the case of slab geometry. The results obtained in both models are discussed in Section 4.

## 2. Pairing with the Gogny force in the hard wall slab potential.

Let us consider a slab of nuclear matter embedded in a hard wall potential of thickness  $2L$  along the  $x$ -direction. Let the origin be at the center of the slab. We start from expanding the gap operator in  $r$ -space  $\Delta(\mathbf{r}, \mathbf{r}')$  in terms of the wave functions  $\varphi_{\mathbf{k}}(\mathbf{r})$  of the hard-wall slab potential,

$$\varphi_{\mathbf{k}}(\mathbf{r}) = \frac{1}{L} \theta(L+x) \theta(L-x) \sin k_x(x-L) e^{i\mathbf{k}_{\perp}\mathbf{r}_{\perp}}, \quad (1)$$

where  $k = \{k_x, \mathbf{k}_{\perp}\}$ , the quantum number  $k_x$  running over the discrete set of eigenvalues  $k_n = \pi n/(2L)$ ,  $n = 1, 2, \dots$ . Within the usual BCS approximation the expansion reads

$$\Delta(\mathbf{r}_1, \mathbf{r}_2) = \sum_{\mathbf{k}} \varphi_{\mathbf{k}}(\mathbf{r}_1) \varphi_{-\mathbf{k}}(\mathbf{r}_2) \Delta(\mathbf{k}), \quad (2)$$

where the state  $|- \mathbf{k}\rangle$  is time-reversed with respect to the state  $|\mathbf{k}\rangle$ . The gap  $\Delta(\mathbf{k})$  obeys

the BCS equation

$$\Delta(\mathbf{p}) = - \sum_{\mathbf{k}} \langle \mathbf{p}, -\mathbf{p} | V | -\mathbf{k}, \mathbf{k} \rangle \frac{\Delta(\mathbf{k})}{2\sqrt{\xi^2(\mathbf{k}) + \Delta^2(\mathbf{k})}}, \quad (3)$$

where  $\xi(\mathbf{k}) = \varepsilon(\mathbf{k}) - \mu$  is the single-particle energy relative to the chemical potential and

$$\langle \mathbf{p}, -\mathbf{p} | V | -\mathbf{k}, \mathbf{k} \rangle = \iint d\mathbf{r}_1 d\mathbf{r}_2 \varphi_{\mathbf{p}}^*(\mathbf{r}_1) \varphi_{-\mathbf{p}}^*(\mathbf{r}_2) V(\mathbf{r}_1, \mathbf{r}_2) \varphi_{-\mathbf{k}}(\mathbf{r}_2) \varphi_{\mathbf{k}}(\mathbf{r}_1) \quad (4)$$

are the matrix elements of the pairing interaction  $V(\mathbf{r}_1, \mathbf{r}_2)$ . For the purpose of performing calculations analytically we used here, as in [2], the Gogny force D1

$$V(\mathbf{r}_1, \mathbf{r}_2) = \sum_{c=1}^2 (W_c - B_c - H_c + M_c) e^{-(\mathbf{r}_1 - \mathbf{r}_2)^2/\alpha_c^2} \quad (5)$$

with the values of the parameters given in [7].

Using the explicit form of the eigenfunctions (1) in Eq. (4) one obtains

$$\begin{aligned} \langle \mathbf{p}, -\mathbf{p} | V | -\mathbf{k}, \mathbf{k} \rangle &= \frac{1}{2L^2} \sum_{c=1}^2 (W_c - B_c - H_c + M_c) \pi \alpha_c^2 e^{-\alpha_c^2(p_{\perp}^2 - k_{\perp}^2)/4} \\ &\times \iint dx_1 dx_2 \theta(x_1 + L) \theta(L - x_1) \theta(x_2 + L) \theta(L - x_2) \\ &\times \sin(k_x(x_1 - L)) \sin(k_x(x_2 - L)) \sin(p_x(x_1 - L)) \sin(p_x(x_2 - L)) e^{-(x_1 - x_2)^2/\alpha_c^2}. \end{aligned} \quad (6)$$

Upon substituting this expression into Eq. (3) and, as the  $s$ -wave pairing is considered, averaging over the angle between vectors  $\mathbf{p}$  and  $\mathbf{k}$ , the gap equation can be rewritten as follows

$$\begin{aligned} \Delta(p_m, p_{\perp}) &= \frac{1}{4L^2} \sum_{c=1}^2 (W_c - B_c - H_c + M_c) \alpha_c^2 e^{-\alpha_c^2 p_{\perp}^2/4} \\ &\times \sum_n \int_0^{\infty} k_{\perp} dk_{\perp} e^{-\alpha_c^2 k_{\perp}^2/4} I_0\left(\frac{\alpha_c p_{\perp} k_{\perp}}{2}\right) \frac{\Delta(k_n, k_{\perp})}{\sqrt{\xi^2(k_n, k_{\perp}) + \Delta^2(k_n, k_{\perp})}} \\ &\times \iint dx_1 dx_2 \theta(x_1 + L) \theta(L - x_1) \theta(x_2 + L) \theta(L - x_2) \\ &\times \sin((k_n(x_1 - L)) \sin(k_n(x_2 - L)) \sin(p_m(x_1 - L)) \sin(p_m(x_2 - L)) e^{-(x_1 - x_2)^2/\alpha_c^2}, \end{aligned} \quad (7)$$

where  $I_0(z)$  is the modified Bessel function.

Integrating then over  $x_1$  and  $x_2$  and introducing the function

$$g_c(p, k) = \frac{i\sqrt{\pi}\alpha_c}{2L^2(p+k)} \left\{ e^{-\alpha_c^2 k^2/4} \left[ \left( e^{2i(p+k)L} + 1 \right) \text{erf}\left(\frac{ik\alpha_c}{2}\right) - \text{erf}\left(\frac{ik\alpha_c}{2} - \frac{2L}{\alpha_c}\right) \right] \right\}$$

$$\begin{aligned}
& -e^{2i(p+k)L} \operatorname{erf}\left(\frac{ik\alpha_c}{2} + \frac{2L}{\alpha_c}\right) \Big] + e^{-\alpha_c^2 p^2/4} \left[ \left( e^{2i(p+k)L} + 1 \right) \operatorname{erf}\left(\frac{ip\alpha_c}{2}\right) \right. \\
& \left. - \operatorname{erf}\left(\frac{ip\alpha_c}{2} - \frac{2L}{\alpha_c}\right) - e^{2i(p+k)L} \operatorname{erf}\left(\frac{ip\alpha_c}{2} + \frac{2L}{\alpha_c}\right) \right] \Big\}, \tag{8}
\end{aligned}$$

we arrive at the gap equation in the following form

$$\begin{aligned}
\Delta(p_m, p_\perp) = & -\frac{1}{2} \sum_{c=1}^2 \alpha_c^2 (W_c - B_c - H_c + M_c) e^{-\alpha_c^2 p_\perp^2/4} \int_0^\infty k_\perp dk_\perp e^{-\alpha_c^2 k_\perp^2/4} I_0\left(\frac{\alpha_c p_\perp k_\perp}{2}\right) \\
& \times \sum_n \frac{\Delta(k_n, k_\perp)}{\sqrt{\xi^2(k_n, k_\perp) + \Delta^2(k_n, k_\perp)}} G_c(p_m, k_n), \tag{9}
\end{aligned}$$

where

$$\begin{aligned}
G_c(p, k) = & \frac{1}{8} \operatorname{Re} \left\{ g_c(p+k, p+k) + g_c(p-k, p-k) + g_c(p+k, -p-k) \right. \\
& \left. + g_c(p-k, -p+k) - 2g_c(p+k, -p+k) - 2g_c(p+k, p-k) \right\}. \tag{10}
\end{aligned}$$

To reveal spatial behavior of the nonlocal pairing gap operator the Wigner transform of the gap is very useful. It reads

$$\Delta(\mathbf{R}, \mathbf{k}) = \int d\mathbf{s} \Delta(\mathbf{R}, \mathbf{s}) e^{i\mathbf{ks}}, \tag{11}$$

where  $\mathbf{R} = (\mathbf{r}_1 + \mathbf{r}_2)/2$  and  $\mathbf{s} = \mathbf{r}_1 - \mathbf{r}_2$ . In the case of slab geometry, the Wigner transform (11) of the gap operator depends only on  $X$  which is the component of  $\mathbf{R}$  perpendicular to the surface. Considering  $\Delta(X, k_x, k_\perp)$  only for  $X > 0$ , since it is an even function of  $X$ , one can easily obtain the following series:

$$\begin{aligned}
\Delta(X, k_x, k_\perp) = & \frac{1}{\pi L} \theta(L-X) \sum_{n=1}^{\infty} \Delta(k_n, k_\perp) \left[ 2 \cos(k_n(X-L)) \frac{\sin(2k_x(X-L))}{k_x} \right. \\
& \left. - \frac{\sin(2(k_x - k_n)(X-L))}{k_x - k_n} - \frac{\sin(2(k_x + k_n)(X-L))}{k_x + k_n} \right]. \tag{12}
\end{aligned}$$

In the bulk, the gap  $\Delta$  depends mainly on the total momentum  $k = \sqrt{k_x^2 + k_\perp^2}$ . Approximately, this is true also for the surface region. Within this approximation, we can treat the gap at the Fermi surface  $\Delta(X, k_F(X))$  as the Wigner transform  $\Delta(X, k_x, k_\perp)$  taken at  $k = k_F(X)$ , where  $k_F = (3\pi^2 \rho(X)/2)^{1/3}$  is the local Fermi momentum. We define the gap-shape function as the gap at the Fermi surface normalized to one at the center of the slab:

$$\chi_F^G(X) = \Delta(X, k_F(X)) / \Delta(0, k_F(0)). \tag{13}$$

The function  $\chi_F^G(X)$  is drawn in Fig. 1 (a and b) for four different values of the half-width of the slab:  $L = 4, 6, 8$  and  $10$  fm. In Fig. 1a the gap-shape function is calculated for the Fermi momentum  $k_F = 1.4232 \text{ fm}^{-1}$  corresponding to the Fermi energy  $\varepsilon_F = 42 \text{ MeV}$ , while in calculation of Fig. 1b the value of Fermi momentum,  $k_F = 1.4894 \text{ fm}^{-1}$ , corresponds to  $\varepsilon_F = 46 \text{ MeV}$ .

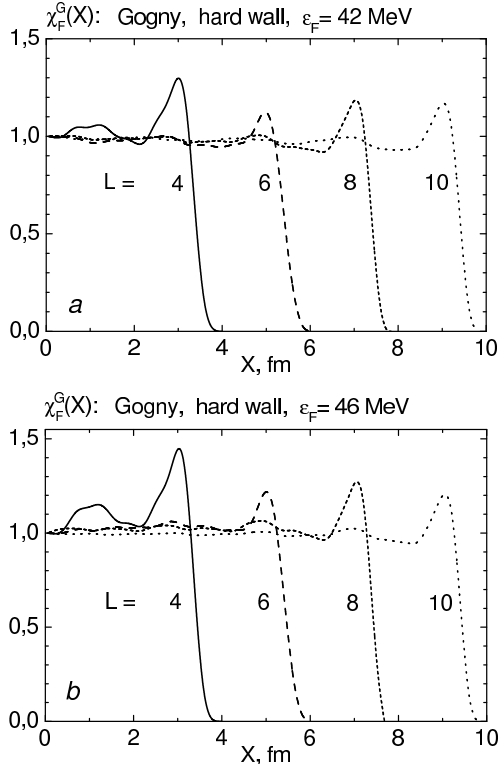


Figure 1: The gap-shape function  $\chi_F^G(X)$  calculated in the model of pairing with the Gogny force in the slab of nuclear matter within the hard wall potential for  $\varepsilon_F = 42$  MeV (panel a) and  $\varepsilon_F = 46$  MeV (panel b). The half-width  $L$  of the slab is given (in fm) by the numbers close to the curves.

values. In fact, in finite nuclei like the tin isotopes, we should look at a great number of nuclei in the isotopic chain because the behavior of  $\Delta(r)$  can fluctuate a great deal passing through the open neutron shell in question.

A detailed study of several long isotopes chains [9] with density dependent effective pairing forces confirmed that, in the framework of a phenomenological approach, it is rather difficult to distinguish between two opposite possibilities, the volume pairing and the pairing with pronounced surface enhancement. For this purpose, the analysis of some binding energy characteristics, such as separation energies, should be accompanied by the study of the variations of nuclear radii along the chain. The odd-even staggering phenomenon is especially sensitive to the coordinate dependence of  $\Delta$ . The microscopic calculation of  $\Delta$  should help to solve this problem.

Of course, the conclusion may strongly depend on the employed pairing force and below we will investigate the surface behavior of pairing with a separable version of the Paris force.

### 3. Pairing with the Paris force in a slab of nuclear matter within a Saxon-Woods potential.

Now we shall adopt the more realistic one-dimensional Saxon-Woods potential  $U(X)$  for a slab with the width of  $2L$  symmetrical around the origin  $X = 0$ :

$$U(X) = \frac{U_0}{1 + \exp((X-L)/d) + \exp(-(X+L)/d)}. \quad (14)$$

Here  $U_0$  is the potential depth in the central region and  $d$  is the diffuseness parameter (to be more exact, the maximum potential depth is  $U(0) = U_0 / (1 + 2 \exp(-L/d))$ ). The two parameters ( $U_0 = -50$  MeV and  $d = 0.65$  fm) are taken to be close to those of real atomic nuclei. The half-width parameter  $L$  will be changed to examine the size dependence of the effect under consideration.

To avoid a rather cumbersome resolution of the Bogolyubov equations for the nonlocal gap [10], as in [1], we use a powerful method [11] (we refer to it as KKC) of solving the gap equation for the case of a nonlocal interaction. This method was originally suggested for infinite matter where the gap  $\Delta$  can be represented as a product  $\Delta(p) = \Delta_F \chi(p)$  of the constant  $\Delta_F = \Delta(p_F)$  and the "gap-shape" function  $\chi(p)$  normalized to  $\chi(p_F) = 1$ . Basically the KKC method is a transformation of the gap equation to a set of two coupled equations: an integral equation for  $\chi(p)$ , which is almost independent of the value of  $\Delta_F$ , and an algebraic equation for the value  $\Delta_F$ . This significantly simplifies the solution of the gap equation in infinite matter. In [1] the extension of the KKC method to nonzero temperatures [11, 12] was used in the case of semi-infinite nuclear matter where the spatial dependence of the gap-shape function was also taken into account. Within the KKC method for infinite matter, the temperature and momentum parts of the gap function can be factorized as follows:  $\Delta(\mathbf{p}, T) = \Delta_F(T) \chi(\mathbf{p})$ . In [1] it was supposed that a similar separation of the temperature factor can be made for the semi-infinite system:

$$\Delta(x_1, x_2, k_\perp^2; T) = \Delta_F(T) \chi(x_1, x_2; k_\perp^2). \quad (15)$$

An additional advantage from using the KKC method in this case comes from the possibility of finding the normalization factor  $\Delta_F(T)$  by solving the gap equation in infinite matter.

In this paper we use the same ansatz (15) for the slab geometry. Unfortunately, in this case no direct relation to infinite nuclear matter exists and there is no evident way to find the normalization factor without solving the Bogolyubov equations. However, since the gap-shape function is of main importance for an analysis of the surface enhancement of the gap, we do not calculate here the normalization factor postponing the solution of the Bogolyubov equation to a forthcoming publication.

As far as in the case of the slab geometry all the equations are very similar to those for semi-infinite matter, we write down explicitly only those which are necessary for explaining our calculations and refer the reader to [1, 6] for details. In symbolic notation, the gap equation has the form [13, 14]:

$$\Delta(T) = \mathcal{V}_{\text{eff}}^p A_0^s(T) \Delta(T) \quad (16)$$

where  $\mathcal{V}_{\text{eff}}^{\text{p}}$  is the effective pairing interaction acting in the model space  $S_0$  in which the superfluid two-particle propagator  $A_0^s$  is defined.

The separable  $3 \times 3$  form [3, 4] of the Paris potential [5] is used

$$V(\mathbf{k}, \mathbf{k}') = \sum_{ij} \lambda_{ij} g_i(k^2) g_j(k'^2), \quad (17)$$

where  $\mathbf{k}$  and  $\mathbf{k}'$  are the relative momenta before and after scattering. The effective interaction has a similar separable form which, in notation of [6], is as follows:

$$\mathcal{V}_{\text{eff}}^{\text{p}}(x_1, x_2, x_3, x_4, k_{\perp}^2, k'^2_{\perp}; E) = \sum_{ij} \Lambda_{ij}(X, X'; E) g_i(k_{\perp}^2, x) g_j(k'^2_{\perp}, x'), \quad (18)$$

where  $E=2\mu$ ,  $X=(x_1+x_2)/2$ ,  $x=x_1-x_2$ , etc., and  $g_i(k_{\perp}^2, x)$  stands for the inverse Fourier transform in the  $x$ -direction of the form factor  $g_i(k_{\perp}^2 + k_x^2)$ . The gap-shape factor can be also written as

$$\chi(x_1, x_2; k_{\perp}^2) = \sum_i \chi_i(X) g_i(k_{\perp}^2, x). \quad (19)$$

After substituting Eqs. (15), (17) – (19) into Eq. (16) at  $T = T_c$  we obtain the following equation for the components  $\chi_i$ :

$$\chi_i(X) = \sum_{lm} \int \int dX_1 dX_2 \Lambda_{il}(X, X_1; E) B_{lm}(X_1, X_2, E; T_c) \chi_m(X_2), \quad (20)$$

where

$$\begin{aligned} B_{lm}(X, X', E; T) = & - \sum_{n_1 n_2} \int \frac{d\mathbf{k}_{\perp}}{(2\pi)^2} \frac{1 - N_{\lambda_1}(T) - N_{\lambda_2}(T)}{E - \varepsilon_{\lambda_1} - \varepsilon_{\lambda_2}} \times \\ & \times G_{n_1 n_2}^l(k_{\perp}^2, X) G_{n_1 n_2}^m(k_{\perp}^2, X'), \end{aligned} \quad (21)$$

$$G_{n_1 n_2}^l(k_{\perp}^2, X) = \int y_{n_1}(X + \frac{x}{2}) g_l(k_{\perp}^2, x) y_{n_2}(X - \frac{x}{2}) dx, \quad (22)$$

$$N_{\lambda}(T) = \left( 1 + \exp \frac{\varepsilon_{\lambda} - \mu}{T} \right)^{-1}, \quad (23)$$

In Eqs. (21) – (23),  $\lambda = (n, \mathbf{k}_{\perp})$ ,  $\varepsilon_{\lambda} = \varepsilon_n + k_{\perp}^2/2m$ ,  $\varepsilon_n$  and  $y_n(x)$  stand for the energies and wave functions, respectively, of the 1-dimensional Schrödinger equation with the potential (14).

Following the recipe of Ref. [6] for the effective interaction  $\mathcal{V}_{\text{eff}}^{\text{p}}$  the propagator  $A_0^s$  embodies all the single-particle states with negative energies only. Thus, the summation over  $n_1, n_2$  and the integration over  $\mathbf{k}_{\perp}$  are limited by the conditions:  $\varepsilon_{\lambda} < 0$ ,  $\varepsilon_{\lambda'} < 0$ .

The coefficients  $\Lambda_{ij}$  obey the set of integral equations

$$\begin{aligned} \Lambda_{ij}(X_{12}, X_{34}; E) = & \lambda_{ij} \delta(X_{12} - X_{34}) + \\ & + \sum_{lm} \lambda_{il} \int dX_{56} B_{lm}(X_{12}, X_{56}; E) \Lambda_{mj}(X_{56}, X_{34}; E), \end{aligned} \quad (24)$$

where  $B_{lm}$  are defined by an expression similar to Eq. (21), but without the temperature factor, including the states  $\lambda_1, \lambda_2$  from the complementary subspace.

To simplify the calculations we used the local potential approximation (LPA) which has turned out to be accurate for semi-infinite nuclear matter [6] and for nuclear slabs [15]. The LPA prescription consists in using for the 2-particle propagator  $B$  of the complementary space the local momentum approximation, very similar to the Local Density Approximation (LDA) [16], for each particle separately:  $\varepsilon_n \rightarrow p_x^2/2m + V(X)$ ,  $\varepsilon_{n'} \rightarrow (p'_x)^2/2m + V(X)$ . This type of approach, where the individual particles are treated in semiclassical approximation was used in [17] for examining the response function. This approximation has been shown to be very accurate, if one is not interested in fine details. It should be stressed that the LPA is only applied to the equation for the effective interaction  $\mathcal{V}_{\text{eff}}^{\text{p}}$ , while no local approximation is used in the renormalized gap equation (16). That is, the local approximation is used only for two-particle states belonging to the complementary space, for which the corresponding energy denominators in eq.(21) are large. Therefore the individual contribution of each state is negligible, and only the sum of a number of such contributions is important. For such a sum the semiclassical and local approximations are expected to be accurate. In this respect LPA is different from the standard LDA, since in the latter the local approximation is used for all two-particle states.

Within the LPA, the exact values of  $B_{lm}(X_1, X_2; E)$  are replaced by the set of  $B_{lm}^{\text{inf}}(t, E; U[X])$  calculated for infinite nuclear matter put into the homogeneous potential well of the depth  $U[X]$ . Here  $t=X_1-X_2$ ,  $X=(X_1+X_2)/2$  are the relative and average values of the CM coordinates. In the first step of the LPA procedure we calculate the set of vectors  $B_{lm}^{\text{inf}}(t, E = 2\mu; U_i)$  ( $V_i = \delta V \cdot (i-1)$ ) for a fixed value of the chemical potential  $\mu$ . In the second step, for each value of  $(X, t)$ , we find  $B_{lm}^{\text{LPA}}(X_1, X_2)$  interpolating the values of  $B_{lm}^{\text{inf}}(t; V_i)$  by the values of  $V_i$  nearest to  $V(X)$ . After substitution of  $B_{lm}^{\text{LPA}}(X_1, X_2)$  into Eq. (24) we find the LPA prescription  $\Lambda_{lm}^{\text{LPA}}(X_1, X_2)$  for the effective interaction which should be substituted into the homogeneous Eq.(20) for the gap-shape function. If the critical temperature  $T_c$  was known, this equation could be solved directly. To find  $T_c$  a more general integral equation must be considered

$$\chi_i(X) = \lambda(T) \sum_{lm} \int dX_1 K_{il}(X, X_1) \chi_m(X_1), \quad (25)$$

which involves the eigenvalue  $\lambda(T)$ . Here the abbreviation  $K = \Lambda B^0$  is introduced for the kernel. The critical temperature can be found from the evident condition  $\lambda(T_c) = 1$ .

The entire calculation scheme is similar to that for semi-infinite matter except for some details. First, in the slab case we are dealing with the discrete spectrum  $\varepsilon_n$  in Eq. (21). Second, due to the obvious reflection symmetry of the slab system in the  $x$ -direction, all the integral equations under consideration can be readily reduced to a form including positive  $X$  only. Just as in [1], instead of the direct solution of Eq. (25) in the coordinate space, we use the Fourier expansion within the symmetrical interval  $(-L_0, L_0)$ ,

$$\chi_i(X) = \sum_n \chi_i^n f_n(X), \quad (26)$$

where only the even functions must be retained,  $f_n(x) = \cos(\pi n(X - X_c)/L_0)$ . The kernels  $K_{ij}(X, X')$  of Eq. (25) are also expanded in a double Fourier series. Finally we arrive at a set of homogeneous linear equations for the coefficients  $\chi_i^n$  :

$$\chi_i^n = \sum_{j=1}^3 \sum_{n'=1}^N K_{ij}^{nn'} \chi_j^{n'}, \quad (27)$$

which can be solved by standard numerical methods. Then the components of the gap-shape function are found from Eq. (26).

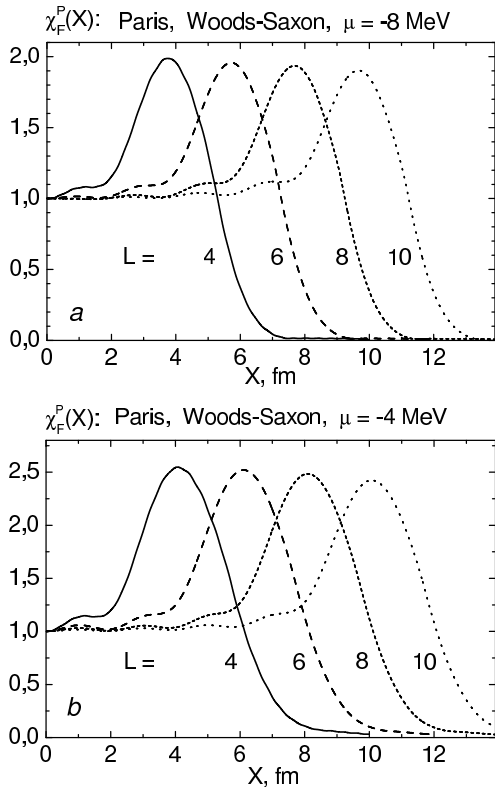


Figure 2: The gap-shape function  $\chi_F^P(X)$  calculated in the model of pairing with the Paris force in the slab of nuclear matter within the Saxon-Woods potential for  $\mu = -8$  MeV (panel a) and  $\mu = -4$  MeV (panel b). The half-width parameter  $L$  is given in the same way as in Fig. 1.

of  $V_0 = -50$  MeV correspond precisely to the Fermi energies  $\varepsilon_F = 42$  MeV and  $\varepsilon_F = 46$  MeV, respectively, of the previous model. Going from  $\mu = -8$  MeV to  $\mu = -4$  MeV a rather important increase of the enhancement of the order of 30% is observed which is much larger

9

Instead of analyzing the separate components  $\chi_i(X)$  for the separable form (17) of Paris force it is more useful to display the local form of the gap-shape function which enters the matrix elements of the gap for states nearby the Fermi surface:

$$\chi_F^P(X) = \sum_i \chi_i(X) g_i(k^2 = k_F^2(X)), \quad (28)$$

where  $k_F(X) = \sqrt{2m(\mu - U(X))}$  is the local Fermi momentum ( $k_F(X) = 0$  for  $\mu - U(X) < 0$ ). We calculated the gap-shape function  $\chi_F^P(X)$  for the same values of the half-width of the slab,  $L = 4, 6, 8$  and  $10$  fm, as in the case of the hard wall potential and for two values of the chemical potential  $\mu = -8$  MeV and  $-4$  MeV. As the depth of the Saxon-Woods potential was taken  $U_0 = -50$  MeV, these two values of  $\mu$  correspond just to the same values of the Fermi energy as in the hard-wall case. The results are shown in Fig. 2 a and b.

One observes a surface bump which is much more pronounced than in the previous model with the Gogny force and the hard wall potential. The enhancement is now around 80% - 100% and, as for the Gogny force, it is quite similar to the semi-infinite matter case [1]. Two values of the chemical potential  $\mu = -8$  MeV and  $\mu = -4$  MeV have been chosen which in account of the depth of the Saxon-Woods potential

than in the case of the hard-wall potential with the Gogny force. On the other hand, there is little variation with the thickness of the slab, the maximum of  $\Delta$  being a couple of percent larger for small slab size. This situation is analogous to the previous model.

The surface effect in  $\Delta$  for the Paris force can be qualitatively explained from the properties of the effective interaction  $\mathcal{V}_{\text{eff}}^{\text{P}}$  which were analyzed in [18]. There it was found that  $\mathcal{V}_{\text{eff}}^{\text{P}}$  undergoes a sharp variation in the surface region, from almost zero in the bulk to very strong attraction in vacuum. In the asymptotic region, the latter coincides with the off-shell  $T$ -matrix of free  $NN$ -scattering  $T(E = 2\mu)$  which exhibits a resonant behavior at small  $E$ . The strong surface attraction and the sharp variation in the surface region are mostly responsible for the surface effect of the gap. The  $\mu$ -dependence of the surface effect can be explained by the increase of the jump  $\delta\mathcal{V}_{\text{eff}}^{\text{P}}$  from inside to outside as  $|\mu|$  is decreasing. There are two reasons for such an increase. The first one is the  $k^2$ -dependence of the form factors in Eqs.(17), (18) leading to a reduction of  $\mathcal{V}_{\text{eff}}^{\text{P}}$  in the inner region with increasing values of  $k_F$ . The second one is a pole-like behavior of  $T(E)$  at small  $E$  which results in an increase of  $\mathcal{V}_{\text{eff}}^{\text{P}}$  with decreasing  $|\mu|$  in the exterior, due to the approach to the virtual pole. One sees that both effects work in the same direction resulting in strengthening the surface effect at small values of  $|\mu|$ .

#### 4. Discussion, and conclusions.

In this work we continued our effort to understand the surface behavior of the nuclear gap. Previous investigations considered semi-infinite nuclear matter embedded in i) a hard wall potential with the Gogny force [2] and ii) a potential of Saxon-Woods shape with the separable version of the Paris force [1]. In both cases a surface enhancement was found but which is relatively modest in view of what one could expect from LDA. In the present study we addressed the question whether finite size effects can strongly alter this situation and repeated the former calculation [1, 2] in a slab configuration.

In the first case of pairing with the Gogny force (D1) within the slab of nuclear matter, the hard wall potential allows to perform most part of calculations analytically. The second rather sophisticated case demanded a lot of numerical effort due to the use of the Paris interaction and the Saxon-Woods shape of the mean field potential. In both cases a noticeable surface effect for the pairing gap was obtained of the same order of magnitude as it was previously found in semi-infinite nuclear matter. The shape of the gap in coordinate space turned out to be qualitatively similar in both cases, with a significant surface enhancement. For the value of the chemical potential  $\mu = -8$  MeV which simulates stable atomic nuclei, the enhancement is of the order of 30% for the first model and is almost 100% for the second one. A general feature of both models is the rather smooth dependence of the enhancement on the slab thickness which is approximately 10% in the first case and only 5% in the second one. In both cases, a  $\mu$ -dependence of the surface effect is found: the enhancement coefficient increases as the absolute value of the chemical potential  $|\mu|$  decreases. The latter effect is more pronounced for the Paris interaction and Saxon-Woods potential reaching 30% with diminishing  $|\mu|$  from 8 MeV to 4 MeV. For the Gogny force and box potential, the

corresponding  $\mu$ -effect is approximately 10%.

To understand in detail the possible common physical origin of this surface enhancement as well as the mentioned differences, it is instructive to consider the gap equation in the form (16) in which  $\Delta$  is expressed in terms of the effective interaction  $\mathcal{V}_{\text{eff}}^{\text{p}}$  given by Eq. (18). Properties of the effective interaction generated by the Paris force were analyzed in [18], where it was found to undergo a sharp variation in the surface region. It is this sharp variation that is mostly responsible for the surface effect in the gap. It is natural that in the case of the hard wall box potential the influence of the surface interaction is smaller which makes the surface enhancement weaker.

The  $\mu$ -dependence of the surface effect is explained by the increase of the jump  $\delta\mathcal{V}_{\text{eff}}^{\text{p}} = \mathcal{V}_{\text{eff}}^{\text{in}} - \mathcal{V}_{\text{eff}}^{\text{ex}}$  with decreasing  $|\mu|$ . This increase is caused by two reasons. The first one is the strong  $k^2$ -dependence of the form factors in Eq.(17) leading to a reduction of  $\mathcal{V}_{\text{eff}}^{\text{in}}$  for the larger values of  $k_F$  in the bulk. The second one is an increase of  $\mathcal{V}_{\text{eff}}^{\text{ex}}$  with decreasing  $|\mu|$  caused by the pole-like behavior of the  $T$ -matrix at small  $E$ . Thus, both reasons jointly work towards making the surface effect stronger at small values of  $|\mu|$ . Qualitatively, the two reasons should work also for Gogny force, but the hard wall potential strongly suppresses the second reason, diminishing the surface effect itself and its  $\mu$ -dependence as well. Finally, it should be mentioned that a large value of the coherence length of pairing which is comparable with the size of the slab makes all the effects under considerations rather smooth. In particular, it results in the weak dependence of the surface enhancement of the pairing gap on the slab thickness.

It is worth to point out that the mechanism of the surface enhancement in  $\Delta$  considered in this paper is different from the one of ref. [19]. The latter is related to a contribution to the effective pairing interaction of the virtual exchange by collective surface vibrations. In a consistent description of the surface behavior of the pairing gap in nuclei these two effects should be considered on equal footing.

This research was partially supported by Grants No. 00-15-96590 and No. 00-02-17319 from the Russian Foundation for Basic Research. Two of the authors (E.E.S. and M.V.Z.) thank INFN (Sezione di Catania and LNS) and Catania University for hospitality during their stay in Catania.

## References

- [1] M. Baldo, U. Lombardo, E. E. Saperstein and M. V. Zverev, Phys. Lett. B 459 (1999) 437;
- [2] M. Farine and P. Schuck, Phys. Lett. B 459 (1999) 444;
- [3] J. Haidenbauer, W. Plessas, Phys. Rev. C 30 (1984) 1822.
- [4] J. Haidenbauer, W. Plessas, Phys. Rev. C 32 (1985) 1424.
- [5] M. Lacombe, B. Loiseaux, J. M. Richard, R. Vinh Mau, J. Côté, D. Pirès and R. de Tourreil, Phys. Rev. C 21 (1980) 861.
- [6] M. Baldo, U. Lombardo, E. E. Saperstein and M. V. Zverev, Nucl. Phys. A 628 (1998) 503.
- [7] J. Déchargé and D. Gogny, Phys. Rev. C 21 (1980) 1668; J. F. Berger, M. Girod, and D. Gogny, Comp. Phys. Comm. 63 (1991) 365.
- [8] M. Kleban, B. Nerlo-Pomorska, J. F. Berger, J. Déchargé, M. Girod, and S. Hilaire, Phys. Rev. C 65 (2002) 024309
- [9] S.A.Fayans, S.V.Tolokonnikov, E.L.Trykov, D.Zawischa, Nucl.Phys. A 676 (2000) 49.
- [10] M. Baldo, U. Lombardo, E. E. Saperstein and M. V. Zverev, Phys. At. Nucl. 62 (1999) 1.
- [11] V. A. Khodel, V. V. Khodel and J. W. Clark, Nucl. Phys. A 598 (1996) 390.
- [12] V. A. Khodel, Phys. At. Nucl. 60 (1997) 1033.
- [13] A. B. Migdal, Theory of Finite Fermi Systems and Properties of Atomic Nuclei (Nauka, Moscow, 1982).
- [14] P. Ring, P. Schuck, The nuclear many-body problem (Springer, Berlin, 1980).
- [15] M. Baldo, U. Lombardo, E. E. Saperstein and M. V. Zverev, Eur. Phys. J. A **13** (2002) 307.
- [16] J. P. Jeukenne, A. Lejeune, and C. Mahaux, Phys. Rep. 25 C (1976) 83.
- [17] P. Guichon, J. Delorme, Phys. Lett. B 263 (1991) 157.
- [18] M. Baldo, U. Lombardo, E. E. Saperstein and M. V. Zverev, Phys. Lett. B 447 (2000) 410.
- [19] F. Barranco, R.A. Broglia, G. Gori, E. Vigezzi, P.F. Bortignon, and J. Terasaki, Phys. Rev. Lett. 83 (1999) 2147.